TOPAS a tool to evaluate the impact of cell geometry and radionuclide on alpha particle therapy

Guerra Liberal, F. D. C., McMahon, S. J., & Prise, K. M. (2021). TOPAS a tool to evaluate the impact of cell geometry and radionuclide on alpha particle therapy. *Biomedical Physics and Engineering Express*, *7*(3), Article 035008. https://doi.org/10.1088/2057-1976/abf29f

Published in:
Biomedical Physics and Engineering Express

Document Version:
Publisher's PDF, also known as Version of record

Biomedical Physics & Engineering Express

ENDORSED BY IPEM Institute of Physics and Engineering in Medicine

PAPER • OPEN ACCESS

TOPAS a tool to evaluate the impact of cell geometry and radionuclide on alpha particle therapy

To cite this article: Francisco D C Guerra Liberal *et al* 2021 *Biomed. Phys. Eng. Express* **7** 035008

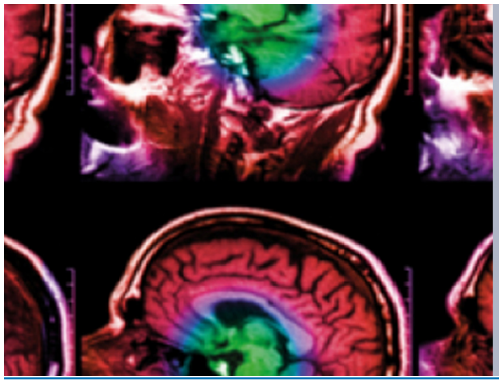

Biomedical Physics & Engineering Express

PAPER

TOPAS a tool to evaluate the impact of cell geometry and radionuclide on alpha particle therapy

Francisco D C Guerra Liberal[1,2], Stephen J McMahon[1] and Kevin M Prise[1]

[1] The Patrick G Johnston Centre for Cancer Research, Queen's University Belfast, 97 Lisburn Road, Belfast, BT9 7AE, United Kingdom
[2] Faculdade de Ciências e Tecnologia, Universidade Nova de Lisboa, 2829-516 Caparica, Portugal

E-mail: francisco.liberal@qub.ac.uk

Keywords: alpha particles, dosimetry, cell geometry, absorbed dose, targeted alpha therapy

Supplementary material for this article is available online

OPEN ACCESS

RECEIVED
20 November 2020

REVISED
1 March 2021

ACCEPTED FOR PUBLICATION
26 March 2021

PUBLISHED
8 April 2021

Abstract

Due to the increasing clinical application of alpha particles, accurate assessment of their dosimetry at the cellular scale should be strongly advocated. Although observations of the impact of cell and nuclear geometry have been previously reported, this effect has not been fully quantified. Additionally, alpha particle dosimetry presents several challenges and most conventional methodologies have poor resolution and are limited to average parameters across populations of cells. Meaningful dosimetry studies with alpha particles require detailed information on the geometry of the target at a subcellular scale. *Methods*. The impact of cellular geometry was evaluated for 3 different scenarios, a spherical cell with a concentric nucleus, a spherical cell with an eccentric nucleus and a model of a cell attached to a flask, consisting of a hemispherical oblate ellipsoid, all exposed to 1,700 ^{211}At radionuclide decays. We also evaluated the cross-irradiation of alpha particles as function of distance to a source cell. Finally, a nanodosimetric analysis of absorbed dose to the nucleus of a cell exposed to 1 Gy of different alpha emitting radionuclides was performed. *Results*. Simulated data shows the dosimetry of self-absorbed-dose strongly depends on activity localization in the source cell, but that activity localization within the source cell did not significantly affect the cross absorbed dose even when cells are in direct contact with each other. Additionally, nanodosimetric analysis failed to show any significant differences in the energy deposition profile between different alpha particle emitters. *Conclusions*. The collected data allows a better understanding of the dosimetry of alpha particles emitters at the sub-cellular scale. Dosimetric variations between different cellular configurations can generate complications and confounding factors for the translation of dosimetric outcomes into clinical settings, but effects of different radionuclides are generally similar.

1. Introduction

Alpha particle-based radionuclides have emerged as an attractive therapeutic option with increased clinical interest since the approval of ^{223}RaCl2 in 2013, after the ALSYMPCA trial [1], as the first alpha emitting radionuclide for the treatment of metastatic castration resistant prostate cancer (mCRPC). This has stimulated clinical interest in other alpha emitting radionuclides, such as astatine-211 (^{211}At), actinium-225 (^{225}Ac) and thorium-227 (^{227}Th) in different clinical settings.

The effectiveness of alpha particles comes from their high LET (60 to 230 keV μm^{-1}), resulting in a dense ionization pattern, that culminates in collections of multiple or complex DSB in close proximity to each other [2]. Despite the increasing interest in alpha particles, their dosimetry presents several challenges and accurate assessments of the dosimetry should be strongly advocated [3, 4]. Meaningful dosimetry studies with alpha particles require detailed information on the geometry of the target on a subcellular scale. Therefore, studying the effects of alpha particles at the sub-cellular level is of interest to determine the suitability of a given radionuclide for targeted radiotherapy., also known as radiopharmaceutical therapy.

The impact of cellular geometry was first identified in 1979 by Lloyd *et al* who showed that from *in vitro*

studies flattened cells can withstand more particle hits due to a variation in the nuclear cross section between spherical and attached cells [5]. Later, Raju *et al* showed that flattened cells needed a higher number of nuclear traversals to be inactivated, due a decrease in the energy deposition per traversal in a thinner nucleus [6].

The effects of cell shape on self-absorbed dose for different radionuclides and monoenergetic electron and alpha particles were previously studied in detail by Goddu *et al*, which has since become a a reference for dosimetry among the medical physics community [7]. Recently, Falzone *et al* reported a significant effect of nucleus eccentricity for Auger electron dosimetry [8]. Similarly, Arnaud *et al* showed major discrepancies between a complex real cell model and a spherical model when exposed to Auger electrons [9]. While it is known that Auger electrons have much smaller ranges than alpha particles tracks, cell specific radiosensitivity and variations in absorbed dose in cell lines with different cellular dimensions have been experimentally shown following exposure to ^{223}RaCl2 [10]. Furthermore, Raghavan *et al* shown significant dosimetric variations among 12 Auger emitters and 2 alpha emitters in a model for the treatment of primary brain cancer [11]. It has been previously demonstrated, by theoretical models, that nucleus size and nuclear geometry can have an impact on the calculated absorbed dose [12].

It is also important to note some previous seminal studies which focus on microdosimetry of single cells exposed to alpha particle emitters such as the ones developed by Goddu *et al* and Stinchmob *et al* [7, 13–15]. In addition, the user-friendly software MIRDcell V2.1 allows a better understanding of the impact of radionuclide choice, activity distribution, cell dimensions and intercellular distances [16]. However, MIRDcell is limited on the number of geometries available, such as 3D clusters in the shape of spheres, ellipsoids, rods and, cones, where all cells and nucleus in the clusters are modelled only as a concentric sphere with the same dimensions. In contrast, TOPAS give the user total freedom to define the desired geometry from a very simple sphere to very complex systems.

The aim of this study was to evaluate the effect of different cellular geometries, cell packing density and energy distribution on the dosimetry of several alpha emitting radionuclides that have clinical potential with the TOPAS Monte Carlo toolkit. Here, we seek to determine whether TOPAS is a valuable alternative to other available software to perform high LET dosimetry at the subcellular scale and enable the investigation of the impact of different cell geometries which are not feasible in other tools. To test this, a Monte Carlo model that simulates alpha particle interactions was applied to 3 different cell geometries. The model takes into account the stochastic nature of alpha particles for a range of clinically relevant macroscopic absorbed doses.

2. Materials and methods

2.1. TOPAS

Dosimetry values were calculated with the TOPAS Monte Carlo modelling tool (version 3.0.1). TOol for PArticle Simulation (TOPAS) is a publicly available MC simulation platform supporting user-friendly dosimetry simulation for research and clinical physicists [17]. TOPAS is a top-level user-friendly software layer over Geant4, which includes the standard Geant4 toolkit, plus additional codes to access Geant4 functionality [18]. TOPAS provides a list of default physics models list that includes: 'g4em-standard_opt4' 'g4h-phy_QGSP_BIC_HP' 'g4decay' 'g4ion-binarycascade' '4h-elastic_HP' and 'g4stopping'. More information about the TOPAS physic list can be found at https://topas.readthedocs.io/en/latest/.

In this study simulations were carried out with 1700 histories, selected as TOPAS isotropic sources with origin and orientation randomly selected inside of the chosen compartment, in 20 independent runs. Emitted alpha particle energies were obtained from the Bureau International des Poids et Mesures 'Table of Radionuclides', as presented in Supplementary table S1 (available online at stacks.iop.org/BPEX/7/035008/mmedia). For each radionuclide, it was assumed that daughters remained in equilibrium with their parent where the complete decay chain was taken into account with the respective emission yield as presented in table S1. Emitted electrons and photons were not included in the calculations [19].

2.2. Influence of cell geometry

The effect of different cell geometries and nuclear positions when exposed to alpha particle irradiation was simulated for 3 different cell models. The deposited dose and number of particle hits at a microscopic level for each individual cellular component were recorded with TOPAS.

The initial model is a spherical cell, consisting of 2 homogeneous spheres of liquid water ($\rho = 1$ g cm^{-3}), representing the cell and its nucleus, immersed in an infinite water medium (figures 1(A)–(B)). Cell (R_C) and nucleus (R_N) radii values used were 10 μm and 5 μm, respectively, representative of cellular dimensions that have been previously used [8]. In the eccentric nucleus model, the nucleus has been translocated 5 μm towards the membrane, such that they touched at one point. Lastly, a model of a cell attached to a flask (figure 1(C)) consists of 1 hemispherical oblate ellipsoid ($a_C = 10$ μm, $b_C = 14.14$ μm, $c_C = 14.14$ μm) of liquid water representing the cell, sitting on a plastic plane with water medium distributed above the plastic plane, and 1 oblate ellipsoid ($a_N = 2.5$ μm, $b_N = 7.07$ μm, $c_N = 7.07$ μm) located inside of the cell, representing the nucleus. The cell parameters are representative values only chosen to simulate dimensions of an average cell and maintain constant volumes between the different simulations.

To evaluate the potential effect eccentricity and sub-cellular geometry could have on dosimetric outcomes, 1700 alpha emitting radionuclides (^{211}At) per cell were distributed (1) uniformly inside the nucleus, (2) uniformly inside the cell cytoplasm but outside the nucleus, (3) exclusively at the cell membrane, and (4) uniformly in the surrounding medium (30 μm around the cell). This number of radionuclides was derived by Chouin *et al* from the activity and number of radiolabelled antibodies per cell as a function of time after injection of 6 MBq of ^{211}At-MX35 within micrometastases from murine models of ovarian carcinoma [20]. It should be noted that, for radionuclides distributed in the medium, the total cross-dose will depend on the activity per unit volume in the medium, and thus the size of the volume simulated in the vicinity of the cell. However, as this work focuses on ratios of dose due to changes in cell geometry, a relatively small volume can be considered without loss of accuracy.

This model took as target compartments: (1) nucleus, (2) cytoplasm and (3) the whole cell. For each scenario, 20 independent runs were simulated to obtain distributions of absorbed doses and decrease uncertainties in their mean values. Based on the TOPAS scorers DoseToMedium, SurfaceTrackCount and EnergyDeposit it was possible to calculate, for each target, the absorbed dose, number of hits and energy deposited, respectively. Here, a hit is defined as when an alpha particle enters a target (cell or nucleus) and stop within or traverses through the target volume and exits, and the absorbed dose was calculated as the sum of energy deposited in the compartment divided by the mass of the compartment.

2.3. Influence of cell geometry

Being aware of the typical nonuniform irradiation profile of alpha-particles, we evaluated the cross-irradiation to neighbouring cells in a concentric model (1 source cell, 14 unlabelled) as a function of the distance to the source cell. These simulations began with the 14 cells placed in a face-centered cubic (fcc) lattice in direct contact with the source cell. This mimics one of the highest cell packing density without overlaps between different cells (fraction of occupied space is 0.74). These simulations were then repeated with increasing membrane to membrane separation from the source cell to neighbouring cells of 0 μm, 5 μm, 10 μm and 20 μm, mimicking a decrease in cellular distribution density (figure 2). 1700 decay events of ^{211}At were distributed in different compartments of the central source cell. Again, the distribution of hits, the absorbed dose and energy deposited were recorded in the cytoplasm, nucleus and whole cell, for each cell in the simulation.

2.4. Physical comparison between different alpha emitting radionuclides

To compare the dose deposition of a range of alpha emitting radionuclides with that of ^{211}At, a nanodosimetric analysis of absorbed dose to the cell nucleus was performed. The nucleus of the concentric cell model (figure 1 A) was used, divided into voxels of 1000 nm^3, and energy deposited in each voxel was recorded. For each simulation, radionuclide decays were randomly distributed in the cellular cytoplasm to generate a cell absorbed dose of 1 Gy, taking into account only the alpha decays of the complete decay chain of each radionuclide (Supplementary table S2). Each scenario and radionuclide was repeated 20 times to obtain a distribution of hits and absorbed doses in the voxels, and decrease uncertainties in their mean values.

2.5. Statistical Analysis

Data were analysed and presented using GraphPad Prism version 7.01 and MATLAB R2017b. Statistical significance was determined using two-way analysis of variance (ANOVA). P values of <0.05 were considered statistically significant

3. Results

3.1. Influence of cell geometry

In figure 3, the absorbed dose to the target and number of hits in each target were calculated for concentric, eccentric and attached cell configurations. Also, the absorbed dose ratio D_{ecc}/D_{conc}, defined as the ratio of the absorbed dose to the target in an eccentric cell

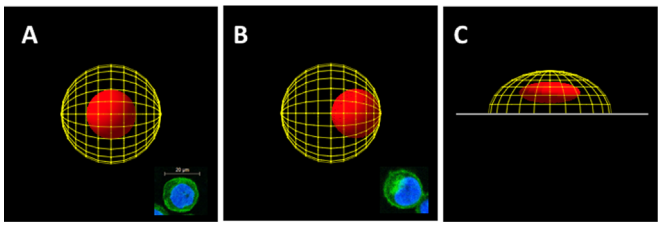

Figure 1. Geometrical models generated with TOPAS (A) concentric (B) eccentric (cell represented in yellow, $R_c = 10\ \mu$m, nucleus represented in red $R_n = 5\ \mu$m) (C) a semi-ellipsoidal cell attached to a flask, (Cell represented in yellow, $a_c = 10\ \mu$m, $b_c = 14.14\ \mu$m, $c_{c.} = 14.14\ \mu$m nucleus represented in red an $= 2.5\ \mu$m, $b_n = 7.07\ \mu$m, $c_n = 7.07\ \mu$m). Inset display cell and nucleus of MDA-MB-468 cell line (A) and H2N (B) with nucleus stained in blue and cytoplasm in green. This research was originally published in JNM, Falzone N, Fernández-Varea JM, Flux G, Vallis KA. Monte Carlo Evaluation of Auger Electron-Emitting Theranostic Radionuclides. J Nucl Med. 2015;56:1441–6. [8].

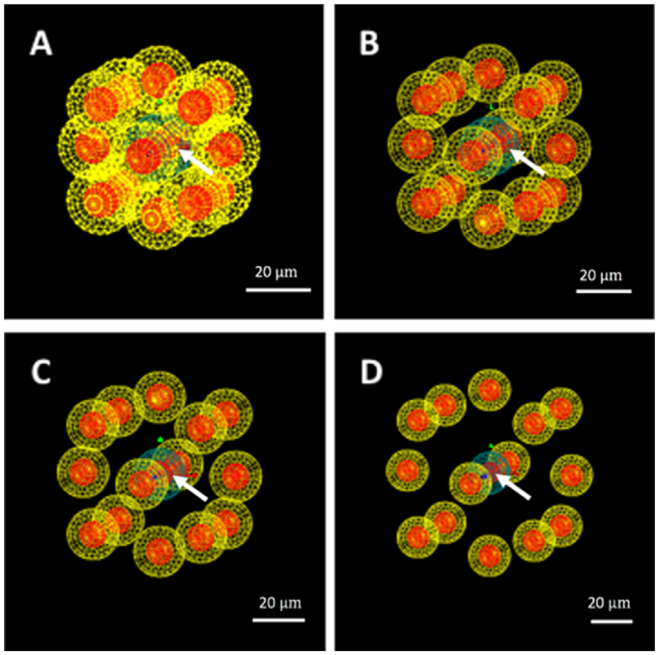

Figure 2. Cluster model with activity uniformly distributed in different compartments of the source cell (green sphere, white arrow) and 14 unlabelled cells (yellow) at different distances from the source cell: (A) 0 μm, (B) 5 μm, (C) 10 μm, (D) 20 μm.

compared with a concentric cell, and the dose ratio $D_{attached}/D_{conc}$, defined as the ratio of the absorbed dose to the target in attached cell compared with a concentric cell, were also quantified. Finally, the hit ratio H_{ecc}/H_{conc} is defined as the ratio of the number of hits in an eccentric cell compared with a concentric cell was assessed.

Figure 3 presents the ratio of the absorbed dose to different targets in an eccentric model compared with a concentric model, together with the hit ratio for uniformly distributed activity of ^{211}At in different source compartments. The evaluation of cellular geometry showed an increased absorbed dose to the nucleus for the eccentric model when the activity is uniformly distributed on the cellular membrane or in the surrounding medium. In contrast, the dose to the nucleus decreases, by 25%, when the activity is distributed at the cytoplasm, as seen in figure 3. Additionally, table 1 shows detailed information on the effect nucleus eccentricity on the energy deposition and hit probability per emitted particle at the nucleus. Moreover, it is important to note that the range of absorbed doses for different hits can be significantly below or above the average dose reported in table 1 (Supplementary figure 2). When emitted from the cell nucleus, each decay will result in a hit to the nucleus (100%). From the cytoplasm, only 13.2% and 10.5% of alpha particles will hit the nucleus for the concentric and eccentric models respectively, while the remaining fraction deposits energy elsewhere. From the cell membrane, the probability of nucleus hits is 6.9% and 11.1% for the concentric and eccentric models respectively. Finally, only 1.4% and 1.6% of the alpha particles will directly intersect the nucleus when emitted from the medium. This last scenario is also dependent on the relative volume of the medium to the cell - here our simulation was carried out considering the distribution of the activity in a volume of a sphere with a radius of 30 μm around the cell.

We also compared self-absorbed dose to the nucleus obtained with TOPAS with two widely accepted scientific methodologies: (1) MIRDcell V2.1 [16] and (2) S-values from the work of Goddu *et al* [7]. Variations between TOPAS and those models are in all simulated scenarios equal or below 10%, which may be attributed to a more detailed energy list for the decay scheme of ^{211}At than the average energies used in this work, and as expected these variations decrease as the distance between the source compartment and the target is increased (table 2).

In the concentric models, the rank order of energy deposited per hit in the nucleus of all investigated configurations was as follows: Medium > Membrane > Cytoplasm > Nucleus. This is because alpha particles incident from greater distances arrive with lower energies and typically higher LETs. However, the probability of hit on the nucleus in both models follows the reverse order. In contrast, in the eccentric models the rank order of energy deposited per hit was as follows: Medium > Cytoplasm > Membrane > Nucleus. This is because the nucleus is now much closer to the membrane than large portions of the cytoplasm, reducing the difference between activity deposited in these two components.

Figure 4 presents a bar plot of the ratio of the absorbed dose to target for the attached cell model compared with a concentric model, for uniformly distributed activity of ^{211}At in different source

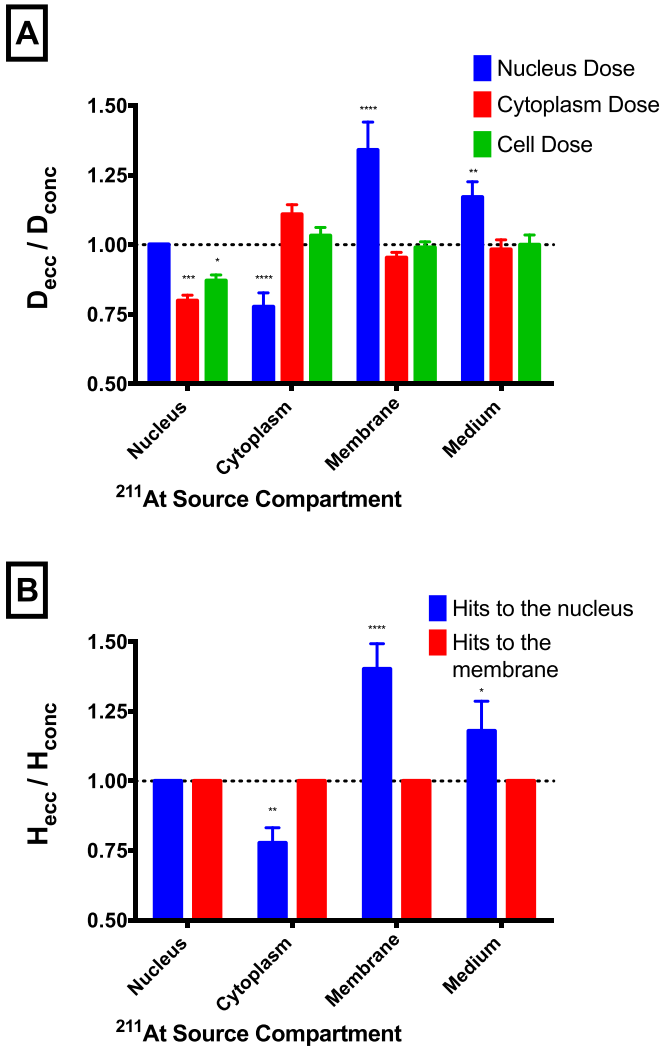

Figure 3. (A) Ratio of absorbed dose to target (D_{ecc}/D_{conc}) in an eccentric model compared with a concentric model for uniformly distributed activity of ^{211}At in different source compartments: nucleus, cytoplasm, membrane and surrounding medium. (B) The relative number of hits is also shown (H_{ecc}/H_{conc}) for ^{211}At. Values represent the average of 20 simulations with the respective standard error. Differences between radionuclide localisation are statistically significant (Two-way ANOVA, $p = 0.0021$), a significant change when compared with the hypothetical value 1 is represented by * ($p < 0.05$), ** ($p < 0.01$), *** ($p < 0.001$), **** ($p < 0.0001$).

compartments. The absorbed dose in the attached cell is, as expected, the same as the absorbed dose in the concentric model when both are exposed to the same activity uniformly distributed in the surrounding medium. ($D_{Attached}/D_{conc} > 0.95$). However, when activity is distributed inside the cell, that is in the nucleus or cytoplasm, the absorbed dose in the cell and its compartments in the in attached model, is reduced in comparison with the concentric model ($D_{Attached}/D_{conc} \approx 0.85$). It is important to state that variables such as, cell and nucleus size will substantially influence the absorbed dose to the nucleus. It has been previously demonstrated that cells with larger cytoplasmatic radii and nuclear to cytoplasm volume ratios have greater alpha particle radiation sensitivity [21]. However, a detailed exploration of such variables are outside the focus of this work,

3.2. Influence of cell packing density

Figure 5 presents the relationship between the average absorbed dose to cells and distance to the source cell. It is possible to observe that the absorbed dose to the nucleus and hits to the cellular and nuclear membranes decreases with distance and that the subcellular localization of the activity in the source cell does not influence the absorbed cross absorbed-dose for any of the evaluated distances (0—20 μm). Additionally, a similar trend of absorbed dose in the cytoplasm and the whole cell is seen as function of the distance to the source cell (Supplementary figure 3).

The absorbed dose and the number of hits obtained for cross-irradiation at different distances from the source in each cell are shown in figure 6. In this scenario the absorbed dose to the nucleus of the source cell is approximately 33 Gy. The absorbed cross absorbed-dose radiation follows an approximately Poisson distribution with a mean of 4.02 Gy and Standard Deviation (SD) of 1.23 Gy, and a coefficient of

Table 1. Eccentricity effect on the deposited energy per hit and on the probability of hits on the nucleus for 1700 decays of ^{211}At. Values represent the average of 20 simulations with the respective standard deviation.

	Concentric Model		Eccentric Model	
Compartment	Dose per hit on nucleus (cGy)	Probability of hit on nucleus (%)	Dose per hit on nucleus (cGy)	Probability of hit on nucleus (%)
Nucleus	8.26 ±0.3	100 ±0.0	8.26 ±0.5	100 ±0.0
Cytoplasm	14.99 ±0.6	13.2 ±0.5	14.69 ±0.9	11.6 ±0.7
Membrane	15.91 ±1.8	6.9 ±0.8	14.07 ±1.5	11.1 ±0.7
Medium	18.36 ±2.7	1.4 ±0.9	18.66 ±2.7	1.6 ±1.0

Table 2. Absorbed dose to the nucleus in the concentric model for 1700 decays of ^{211}At by three different approaches (1) TOPAS; (2) MIRDcell; and (3) Goddu's S-values when activity is uniformly distributed in the nucleus (N → N), cytoplasm (C → N) or cell membrane (M → N), with the percentage of variation between the MIRDcell and S-values to TOPAS expressed in brackets.

	TOPAS	MIRDcell	S-values Goddu
N → N	140.4 Gy	154 Gy (9.7%)	136.0 Gy (3.1%)
C → N	33.6 Gy	32.3 Gy (3.9%)	31.4 Gy (6.5%)
M → N	17.7 Gy	17.9 Gy (4.3%)	17.2 Gy (2.8%)

variation of 31%, when the cells are in direct contact with the source cell (0 μm), (figure 6(A)), and mean of 1.10 Gy and SD of 0.75 Gy, and a coefficient of variation of 61% when the cell membranes are 20 μm away from the membrane of the source cell. In this situation ~3% of cells do not absorb any dose (figure 6 B). Once again, these values are in good agreement with MIRDcell simulations where cross-dose from cells exposed to the same activity at equivalent distances will have an absorbed dose of 6.78 Gy when cells are in direct contact with the source cell and 1.19 Gy when cell membranes are 20 μm away from the membrane of the source cell. As mentioned before these differences in absorbed dose can be attributed to the more detailed decay scheme of MIRDcell software. Interestingly, changing from the default TOPAS physics models to a modular list which uses the low-energy 'g4em-penelope' instead of the standard physics, which is optimized for higher energy particles, increases the absorbed dose to the nucleus when cells are in direct contact in our simulations to a value in closer agreement with MIRDcell (5.46 Gy TOPAS versus 6.78 Gy MIRDcell). Replacing these physics lists with the very low-energy Geant4-DNA physics lists may further improve agreement, however this comes with a substantial cost in computational power.

Similar variations to the number of hits to the nucleus of cells exposed to a uniform distribution of alpha sources have been also reported by Humm, where such variation follows a Poisson distribution and the average hit number is dependent on the radionuclide activity at the target to [22].

In these figures cell-to-cell fluctuations in absorbed dose and hits to the nucleus is also evident. Despite all 14 cells being located at the same distance from the source cell, there is a nonuniform profile of the absorbed doses and hits on the cell membrane and nucleus. Moreover, it is clear that different hits to the nucleus can deposit different energies. For example, cells 7, 8 and 9 in figure 6(D) have the same number of hits to the nucleus, but different absorbed doses.

3.3. Physical comparison between different alpha emitting radionuclides

For the simulated conditions 99.9% of the voxels within the nucleus see 0 deposited energy, and this is independent of the chosen radionuclide. Figure 7(A) shows the fractional probability distribution for energy deposited in voxels (1000 nm^3) with absorbed energy different from zero for different alpha emitters, when activity is randomly distributed in the cellular cytoplasm, this is, voxels with zero absorbed energy were not taken into account. Detailed analysis of the energy distribution on a subcellular scale fails to show any substantial differences between different radionuclides when only the energy and number of alpha particles emitted per radionuclide are considered.

In addition, these analyses show that it is highly improbable for a voxel to be hit by more than one alpha particle at clinically relevant activities.

Additionally, figures 7(B) and (C) display a comparison of the ratio of the absorbed dose to the nucleus among different alpha emitting radionuclides and cell models as previously described. Once again, all alpha emitting radionuclides have the same behavior, with absorbed dose to the nucleus in the eccentric model around 25% and 50% higher than in the concentric model when activity is distributed in the surrounding medium and cellular membrane respectively, and always slightly lower when distributed in the cytoplasm. A similar trend is observed between the attached and concentric model when the activity is distributed in the membrane, medium or in cytoplasm, but there are also variations in this absorbed dose ratio when activity is distributed in the nucleus, the absorbed dose in the attached model is around 10% lower than in the concentric model when activity is distributed in the nucleus. These variations are significant between models ($P < 0.0001$ 2-way ANOVA) and marginally statistically significant between radionuclides ($P = 0.033$ 2-way ANOVA). However, it should be noted that although it is statistically

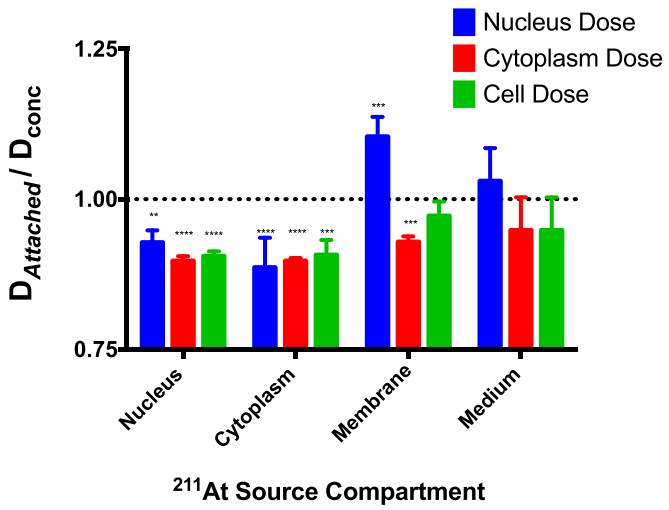

Figure 4. Ratio of the absorbed dose to target ($D_{Attached}/D_{conc}$) in a cell attached to a flask model compared with a concentric model for uniformly distributed activity of ^{211}At in different source compartments, namely nucleus, cytoplasm, membrane and surrounding medium. Values represent the average of 20 simulations with the respective standard error. Differences between radionuclide localisation are statistically significant (Two-way ANOVA, p=0.0038), a significant change when compared with the hypothetical value 1 is represented by * ($p < 0.05$), ** ($p < 0.01$), *** ($p < 0.001$), **** ($p < 0.0001$).

significant within these simulations, the magnitude of the differences between radionuclides is on the order of a few percent, likely smaller than differences in uptake and distribution between the isotopes.

It is also important to highlight that to obtain absorbed dose to the nucleus of 1 Gy, will require different numbers of decays due the different decay schemes of each radionuclide in study. For radionuclides that only emits a single alpha particle (^{211}At, ^{212}Bi and ^{213}Bi) per decay, 1 Gy is obtained with 80 to 90 decays of the radionuclide in the cytoplasm. However, this number is smaller for radionuclides with multiple alpha particle emissions, such as 19 for ^{223}Ra and ^{225}Ac and 14 for ^{227}Th (Supplementary Table S2).

4. Discussion

Despite the remarkable advances in alpha particle dosimetry and imaging, there is still much debate around its accuracy at a cellular scale and how it can be translated to clinical settings. In this work, the dosimetry of alpha particles at a sub-cellular level in clinically relevant scenarios was investigated using computational modelling in different cell geometries.

Self-absorbed dose to the nucleus simulated by TOPAS are in good agreement with the values obtained with two other well accepted approaches (MIRDcell and S-values from Goddu *et al*), with variations equal or less than 10%. These discrepancies can be attributed to the different energies used in this study (5.87 MeV - 42% branching ratio and 7.45%–58% branching ratio) compared with the more detailed decay scheme of MIRDcell software and the monoenergetic alpha particle used in Goddu *et al* work (7.0 MeV). These variations between our data and other models tend to decrease as the distance between the source compartment and the target compartment increases, as the S-values for different compartments coalesce with distance.

The effects of cell packing density were also evaluated. The evaluation of cellular geometry showed an increased absorbed dose to the nucleus for the eccentric model when the activity is uniformly distributed on the cellular membrane or in the surrounding medium. In contrast, the dose to the nucleus decreases, when the activity is distributed at the cytoplasm. Regardless of the targeting strategy adopted, the cellular geometry can influence the mean absorbed dose to the nucleus and thus the biological effect of a therapeutic agent [8]. Similar conclusions were previously demonstrated by Nettleton *et al*, who noted differences between S values, that is, the specific absorbed dose per cumulated activity (Gy/Bq.s) in spherical and ellipsoid cell geometries [23].

Interestingly, a similar trend is observed for the comparison of the absorbed dose between the attached model with the concentric model. An increased absorbed dose to the nucleus is observed for alpha particles emitted from the cellular membrane or surrounding medium and a decreased effect when alpha particles are emitted inside of the cell when compared with a spherical cell, with variations up to 17% (Two-way ANOVA, p=0.004 compared with a constant ratio of 1) (figure 4).

This phenomenon was first reported by Lloyd *et al* who showed that in *in vitro* studies flattened cells can withstand more particle hits due to a variation in the nuclear cross section between spherical and attached cells [5]. Later, Raju *et al* in seminal work with alpha particles showed that the mean number of alpha particle transversals required to induce a lethal lesion was not constant among all cells, and flattened cells needed

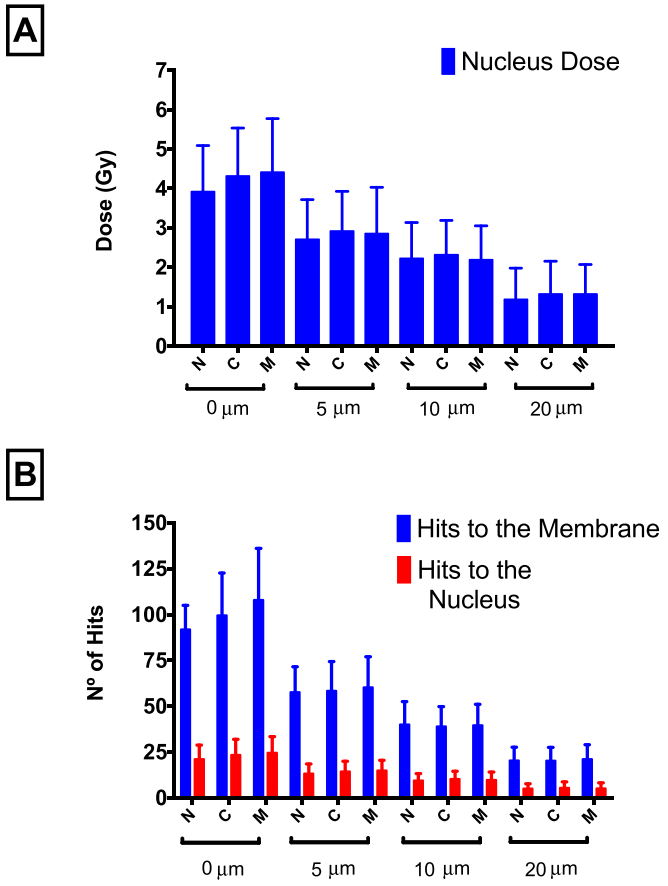

Figure 5. Relationship between the (A) average absorbed dose on the nucleus and (B) hits to cells for different source compartments as a function of the distance (μm) to the source cell when the central cell is exposed to 1700 decays of ^{211}At. X-axis refers to source components defined as: N - activity distributed in the nucleus of labelled cell, C - activity distributed in the cytoplasm of the labelled cell, M - activity distributed in the cellular membrane of labelled cell. Bars represent the average absorbed dose in 14 un-labelled cells in 10 independent simulations with the respective standard error.

a higher number of nuclear hit transversals to be inactivated, due a decrease on the energy deposition per transversal across a thinner nucleus [6, 24]. Recently, Arnaud *et al* showed major discrepancies between a complex real cell model and a spherical model when exposed to Auger electrons, highlighting the importance of modelling geometries as close as possible to the real scenarios [9].

Recently 6% variations in absorbed doses to the whole cell were reported [10] for different cell lines exposed to the exactly same irradiations conditions due to geometric variations in these cell lines. These experimental observations correlate well with the variations found between our three different cell models in silico. Additionally, variations between different cellular configurations, specifically between the spherical cell model and the cell attached to a flask model, a so called geometrical effect can generate complications and confounding factors for the translation of dosimetric evaluations to clinical settings.

Furthermore, absorbed dose is not only dependent on the target cell geometry, but deposition sites of the radionuclide within the cell are another important factor to consider during therapeutic applications, as described by Roeske and Thomas [25] and Goddu *et al* [26]. These dosimetric variations resulting from the impact of intracellular localization are easily available in MIRDcell software [16].

Dose deposition by alpha particles has variations along their tracks, as the LET of alpha particles in the first few microns of their track is lower than when near the Bragg peak. That is, for comparable paths across the cell nucleus, alpha particles that are emitted from the cell membrane or from the medium will deposit more energy than those emitted from the nucleus. Additionally, the average path lengths traversed in the nucleus are generally shorter for alpha particles originating in the nucleus than when originating from the cell surface or medium [25]. This is accounted in analytic dosimetric models as well as for the different Monte Carlo codes available. As it is observed in our results, where the absorbed dose to the nucleus from an alpha particle localized in the cell nucleus (8.26 $\pm$ 0.3 cGy) is less than the absorbed dose when the alpha particle is distributed outside the nucleus (15. $\pm$ 0.1 cGy) (cytoplasm, membrane or medium).

However, to infer the real effectiveness of localized alpha therapy, it is necessary to consider the probability of a hit per emitted particle for different source compartments (table 1). Absorbed dose variations and

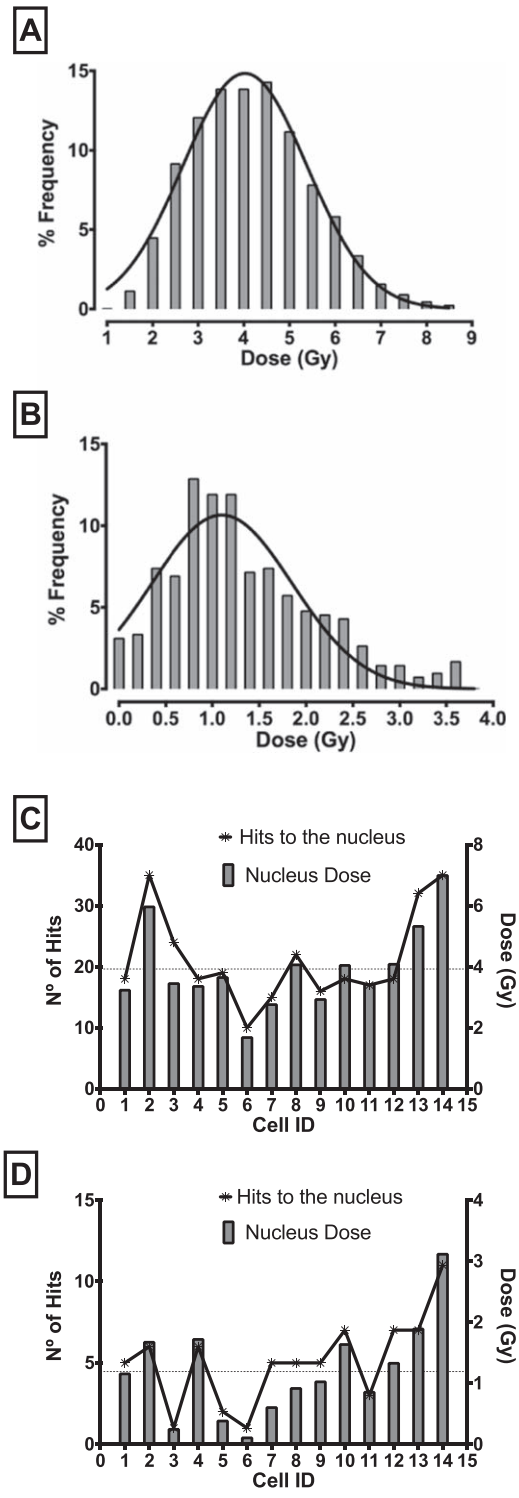

Figure 6. Histogram of the average absorbed dose (Gy) to the nucleus of a cell at different distances after cross-irradiation from a central cell. (A) 0 μm, (B) 20 μm, following 1700 ^{211}At decays in the cytoplasm of the source cell for 10 independent simulations, fitted to a Gaussian distribution; Distribution of nucleus absorbed dose and hits in individual cells at a distance of (C) 0 μm, (D) 20 μm from source cell.

different hit probabilities indicate a strong dependence of self-absorbed-dose dosimetry calculations on activity localization within the source cell.

Charlton showed very little dependence on the activity distribution on the fraction of cells surviving in a 3D spheroid when uniformly exposed to ^{211}At. But in contrast, the cellular distribution density and size of the cluster had a large contribution to the fraction of cells surviving [27].

This can be attributed to the short path length of alpha particles there is a diminished cross absorbed dose, increasing the need to effectively target all cells in the tumour to achieve a uniform distribution of the absorbed dose in the target. Moreover, data presented here shows that activity localization within the source cell does not significantly affect the cross absorbed-dose even when cells are in direct contact with each other, figure 5. This is in good agreement with the work of Goddu *et al*, that cross absorbed-dose plays a diminished role in a cluster of cells if only 10% or less cells are labelled, without significant differences for different cellular compartments (cytoplasm or nucleus) [26].

This, nonuniform distribution of the radiopharmaceutical has been demonstrated in pre-clinical trials with alpha emitting radionuclides, meaning this may be an important consideration for future optimisation [28, 29].

Here different cross-irradiation scenarios were simulated to understand the behavior of absorbed dose distribution among cells exposed to identical source cells. Despite cells being exposed to identical conditions there is a significant variation in the absorbed dose per cell, not only because different cells will experience different number of hits with some cells having multiple hits while other might receive no hits at all, but also because not every particle hit will deposit the same energy, as previously explained.

In the scenario of 20 μm separation between the membrane of the source cell and the unlabelled cells the average absorbed dose is 1.23 Gy with a coefficient of variation of 61%, and in this situation ~3% of cells do not absorb any dose. Humm showed in their microdosimetric model that in a highly nonuniform radioactivity distribution scenario, such as when radioactivity is retained in the capillary, only cells near them will be directedly affected by the alpha particles, and a significant proportion of cells, those away from the capillary receive no hits, regardless of the specific activity used [22]. Similar results have also been previously reported [27, 30–32]. These reports indicate that alpha emitter exposures are likely to lead to highly heterogeneous absorbed dose distributions with a highly localized absorbed dose around targeted cells. But this means that its efficacy in such heterogeneous activity distribution scenarios may be dependent on a second order mechanism such as the bystander effect or tumour anti-vascular therapy, not taken into consideration in these simulations [33, 34].

There are several alpha emitting radionuclides with potential for clinical application and researchers within the field are trying to progress toward a more specific and effective targeted alpha therapy with ^{225}Ac-PSMA as an alternative to ^{223}Ra [35]. A

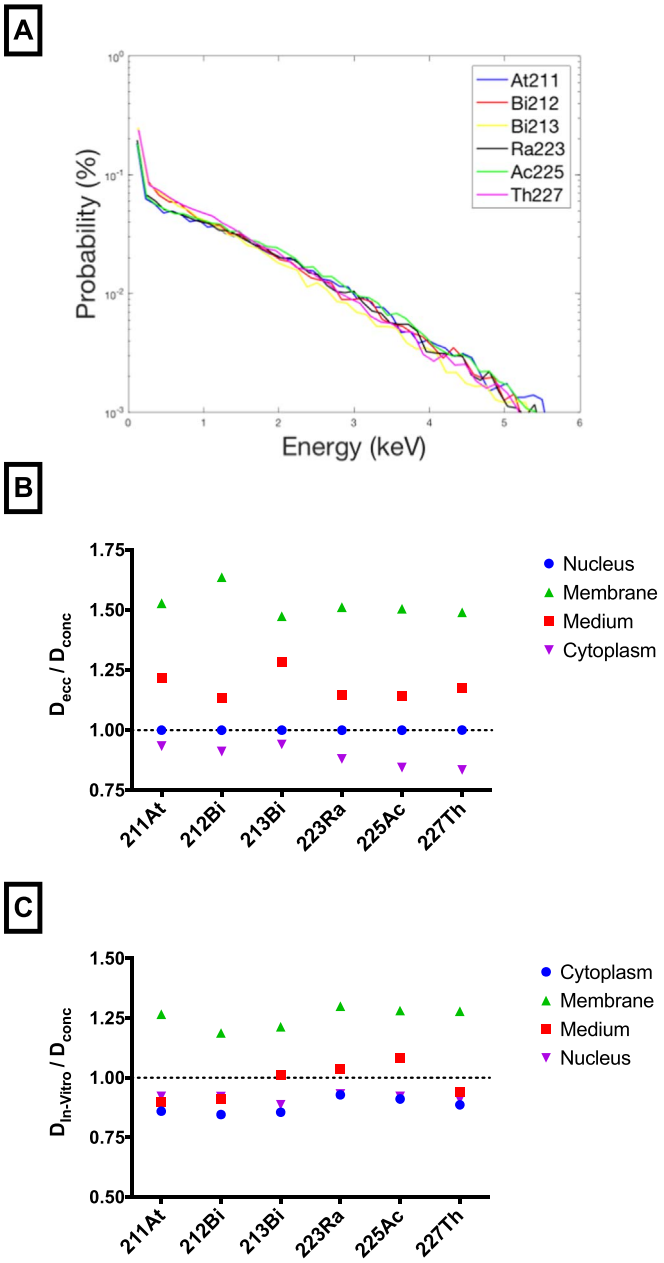

Figure 7. (A) Probability of energy deposition (keV) of different radionuclides (^{211}At, ^{212}Bi, ^{213}Bi, ^{223}Ra, ^{225}Ac and ^{227}Th) in a nucleus sub-divided into 1000 nm^3 voxels, when the cell has an absorbed dose of 1 Gy with activity uniformly distributed in cytoplasm; B) Comparison of the ratio of absorbed dose to nucleus between the eccentric model and the concentric model (D_{ecc}/D_{conc}) for uniformly distributed activity in the nucleus, cytoplasm, membrane and surrounding medium for different radionuclides or C) between the attached model and the concentric model ($D_{In-Vitro}/D_{conc}$). Standard errors are too small to be plotted.

comparative study among different alpha emitting radionuclides in identical conditions is timely and of interest to the community. In a dosimetric analysis at the microscopic level, it was observed that when different radionuclides are used with the same initial spatial activity distribution, there was no significant difference in how they deposited energy on the sub-nucleus scale (figure 7). These results suggest that the exact energy distribution of generated alpha particles does not significantly impact on biological effects, in contrast to recently published observations on Auger emitters [8].

A closer look at the ratios of the absorbed dose to the nucleus between the three different cell geometry models for activity distributed in different compartments within the cell showed that the cell geometry effect was radionuclide independent, that is, variations follows the same trends no matter the chosen radionuclide. While the differences between radionuclide were statistically significant, their magnitude was on the order of a few percent, likely smaller than differences in up-take and distribution which are not included in this model. This analysis was based on the assumption that primordial alpha emitting radionuclide and their progeny will decay in the same

compartment and that there is no diffusion of these radionuclides between compartments between successive decays. This is a reasonable estimate as animal studies have demonstrated little redistribution of ^{223}Ra daughters away from the original tissue compartment [36, 37]. Moreover, in an interesting study by Howell and colleagues, a good correlation was observed between experimental data and an empirical model to calculate possible biological effects of ^{223}Ra and its daughters, without redistribution of ^{223}Ra daughters [38]. However, in some particular scenarios, the detachment of daughters from the targeting carrier can occur due to the recoil energy upon alpha decay having more than sufficient energy to destroy any chemical bond. This would allow the daughter nuclides to diffuse away, leading to energy deposition elsewhere in the surrounding tissues, which is an important aspect that should be taken into account in future studies. Another important aspect to take into account is the physical half-life of the daughter products, as long half-lives will allow these new free radionuclides to diffuse away from the target and therefore contribute to radiation toxicity.

As no significant differences are detected between different alpha particle emitters when only physical aspects of the emitted alpha particles are taken into account, the selection of the ideal alpha emitting radionuclide should be based on chemical and biological properties for targeting and conjugation, availability and physical half-life. Different radionuclides have different decays schemes and consequently different numbers of alpha particle emissions. Radionuclides with multiple alpha particle emissions will need fewer atoms to be delivered to the target than radionuclides with a single alpha particle emission.

The physical half-life of the radionuclide as well as the pharmacokinetics of the radionuclide (biological uptake at the target and clearance half-times) plays a vital role in achieving an effective accumulated absorbed dose per unit time, as different half-lives imply different doses rates for the same accumulated activity at the target, the possible impact of physical half-life and pharmacokinetics are further debated by Raghavan *et al* [11]. For instance, a shorter half-life could achieve larger doses per unit of time when paired with good pharmacokinetics. This is critically important if the surviving cells in the irradiated volume are continuously proliferating [39, 40]. Additionally, physical half-life has a major importance in the industrial logistics of production and distribution, where a very short physical half-life implies a significant waste of activity during transportation.

5. Conclusions

This study evaluates the effect of cellular geometry on self-absorbed-dose and cross-dose with alpha irradiation from different radionuclides using the same conditions. Our simulations take into consideration the stochastic nature of alpha particles at typical clinical doses using the TOPAS Monte Carlo toolkit. The presented data allowed a better understanding of the dosimetry of alpha particles at the sub-cellular scale. Simulated data obtained in this study are in good agreement with values from two more widely accepted approaches, namely MIRDcell and S-values from Goddu *et al*, and helps to support a strong dependence of activity localization in the source cell to self-absorbed-dose dosimetry. However, activity localization within the source cell does not significantly affect the cross absorbed-dose even when cells are in direct contact with each other.

Our results correlate with previous reports from alpha particle therapy suggesting a heterogeneous absorbed dose distribution within the target and a highly localized dose deposition. Moreover, we report no significant differences in the energy deposition profile between different alpha particle emitters, as even for very different numbers of decays required between radionuclides to have an absorbed dose to the cell of 1 Gy. As the clinical implementation of TAT is increasing, this type of analyses may be useful in interpreting future clinical results.

Acknowledgments

The authors gratefully acknowledge the support of Fundação para a Ciência e Tecnologia (FCT-MCTES), Radiation Biology and Biophysics Doctoral Training Programme (RaBBiT, PD/00193/2012); Applied Molecular Bioscience Unit (UCIBIO) (UIDB/04378/2020) and Centre of Physics and Technological Research Unit (CEFITEC) (UIDB/00068/2020); and scholarship grant number SFRH/BD/114448/2016 to (F.D.C.G.L.). The work was funded by the Movember Prostate Cancer UK Centre of Excellence (CEO13_2-004) and the Research and Development Division of the Public Health Agency of Northern Ireland (COM/4965/14).

Data availability statement

All data that support the findings of this study are included within the article (and any supplementary files).

ORCID iDs

Francisco D C Guerra Liberal https://orcid.org/0000-0002-7917-8578
Stephen J McMahon https://orcid.org/0000-0001-5980-6728

References

[1] Parker C *et al* 2013 Alpha emitter radium-223 and survival in metastatic prostate cancer *N. Engl. J. Med.* **369** 213–23

[2] Sgouros G *et al* 2010 MIRD Pamphlet No. 22 (Abridged): radiobiology and dosimetry of alpha-particle emitters for targeted radionuclide therapy *J. Nucl. Med.* **51** 311–28

[3] Gholami Y, Zhu X, Fulton R, Meikle S, El-Fakhri G and Kuncic Z 2015 Stochastic simulation of radium-223 dichloride therapy at the sub-cellular level *Phys Med Biol* **60** 6087-96

[4] Roeske J C and Hoggarth M 2007 Alpha-particle Monte Carlo simulation for microdosimetric calculations using a commercial spreadsheet *Phys. Med. Biol.* 52

[5] Lloyd E L, Gemmell M A, Henning C B, Gemmell D S and Zabransky B J 1979 Cell survival following multiple-track alpha particle irradiation *Int J Radiat Biol Relat Stud Physics, Chem Med* **35** 23-31

[6] Raju M R, Eisen Y, Carpenter S and Inkret C 1991 Radiobiology of alpha particles. III. Cell inactivation by alpha-particle traversals of the cell nucleus *Radiat. Res.* **128** 204–9

[7] Goddu S M, Howell R W, Bouchet L G, Bolch W E and Rao D V 1997 *MIRD cellular S. values: self-absorbed dose per unit cumulated activity for selected radionuclides and monoenergetic electron and alpha particle emitters incorporated into different cell compartments* (Reston, VA: Society of Nuclear Medicine) 183p

[8] Falzone N, Fernández-Varea J M, Flux G and Vallis K A 2015 Monte Carlo evaluation of auger electron-emitting theranostic radionuclides *J Nucl Med* **56** 1441–6

[9] Arnaud F X, Paillas S, Pouget J P, Incerti S, Bardiès M and Bordage M C 2016 Complex cell geometry and sources distribution model for Monte Carlo single cell dosimetry with iodine 125 radioimmunotherapy *Nucl Instruments Methods Phys Res Sect B Beam Interact with Mater Atoms* **366** 227–33

[10] Bannik K *et al* 2019 Radiobiological effects of the alpha emitter Ra-223 on tumor cells *Sci. Rep.* **9** 1–11

[11] Raghavan R, Howell R W and Zalutsky M 2017 A model for optimizing delivery of targeted radionuclide therapies into resection cavity margins for the treatment of primary brain cancers *Biomed. Phys. Eng. Express* **3** 035005

[12] Roeske J C and Stinchcomb T G 2000 Tumor control probability model for alpha-particle-emitting radionuclides *Radiat. Res.* **153** 16–22

[13] Thomas S and Roeske J C 1999 Values of 'S', $\langle z\,1\rangle$, and $\langle z\,1\,2\rangle$ for dosimetry using alpha-particle emitters *Med. Phys.* **26** 1960–71

[14] Goddu S M, Howell R W and Rao D V 1994 Cellular dosimetry: absorbed fractions for monoenergetic electron and alpha particle sources and s-values for radionuclides uniformly distributed in different cell compartments *J. Nucl. Med.* **35** 303–16

[15] Stinchcomb T G and Roeske J C 1992 Analytic microdosimetry for radioimmunotherapeutic alpha emitters *Med. Phys.* **19** 1385–93

[16] Vaziri B *et al* 2014 MIRD pamphlet No. 25: MIRDcell V2.0 software tool for dosimetric analysis of biologic response of multicellular populations *J. Nucl. Med.* **55** 1557–64

[17] Perl J, Shin J, Schümann J, Faddegon B and Paganetti H 2012 TOPAS: an innovative proton Monte Carlo platform for research and clinical applications TOPAS: an innovative proton Monte Carlo platform for research and clinical applications *Med. Phys.* **39** 6818-37

[18] Agostinelli S *et al* 2003 Geant4 - a simulation toolkit. nucl instruments methods phys res sect a accel spectrometers *Detect Assoc Equip.* **506** 250–303

[19] Bé M *et al* 2008 *Table of radionuclides* 1-6 (France: Bur Int des Poids Mes)

[20] Chouin N *et al* 2013 *Ex vivo* activity quantification in micrometastases at the cellular scale using the alpha-camera technique *J. Nucl. Med.* **54** 1347–53

[21] Yard B D, Gopal P, Bannik K, Siemeister G, Hagemann U B and Abazeed M E 2019 Cellular and genetic determinants of the sensitivity of cancer to α-particle irradiation *Cancer Res.* **79** 5640–51

[22] Humm J L 1987 A microdosimetric model of astatine-211 labeled antibodies for radioimmunotherapy *Int. J. Radiat. Oncol. Biol. Phys.* **13** 1767–73

[23] Nettleton J and Lawson R 1996 Cellular dosimetry of diagnostic radionuclides for major spherical and ellipsoidal geometry *Phys. Med. Biol.* **41** 1845–54

[24] Raju M R, Eisen Y, Carpenter S, Jarrett K and Harvey W F 1993 Radiobiology of alpha particles. III. Cell Inactivation by alpha-particle of energies 0.4–3.5 MeV *Radiat. Res.* **133** 289–96

[25] Roeske J C and Thomas S 2006 The average number of alpha-particle hits to the cell nucleus required to eradicate a tumour cell population *Phys. Med. Biol.* 51

[26] Goddu S M, Rao D V and Howell R W 1994 Multicellular dosimetry for micrometastases: dependence of self-dose versus cross-dose to cell nuclei on type and energy of radiation and subcellular distribution of radionuclides *J. Nucl. Med.* **35** 521–30

[27] Charlton D E 2000 Radiation effects in spheroids of cells exposed to alpha emitters *Int. J. Radiat. Biol.* **76** 1555–64

[28] Akudugu J M, Neti P V S V and Howell R W 2011 Changes in lognormal shape parameter guide design of patient-specific radiochemotherapy cocktails *J. Nucl. Med.* **52** 642–9

[29] Neti P V S V and Howell R W 2006 Log normal distribution of cellular uptake of radioactivity: implications for biologic responses to radiopharmaceuticals *J. Nucl. Med.* **47** 1049–58

[30] Hobbs R F *et al* 2012 A bone marrow toxicity model for 223 Ra alpha-emitter radiopharmaceutical therapy *Phys. Med. Biol.* **57** 3207–22

[31] Gholami Y, Zhu X, Fulton R, Meikle S, El-Fakhri G and Kuncic Z 2015 Stochastic simulation of radium-223 dichloride therapy at the sub-cellular level *Phys. Med. Biol.* **60** 6087–96

[32] Elgqvist J *et al* 2006 Alpha-radioimmunotherapy of intraperitoneally growing OVCAR-3 Tumors of variable dimensions: outcome related to measured tumor size and mean absorbed dose *J. Nucl. Med.* **47** 1342–51

[33] Ladjohounlou R *et al* 2019 Drugs that modify cholesterol metabolism alter the p38/JNK-mediated targetedand nontargeted response to alpha and auger radioimmunotherapy *Clin. Cancer Res.* **25** 4775–90

[34] Leung C N *et al* 2020 Dose - dependent growth delay of breast cancer xenografts in the bone marrow of mice treated with radium - 223: the role of bystander effects and their potential for therapy *J. Nucl. Med.* **61** 89–95

[35] Liberal F D C G, O'Sullivan J M, McMahon S J and Prise K M 2020 Targeted alpha therapy: current clinical applications *Cancer Biother Radiopharm.* 1–14

[36] Henriksen G, Fisher D R, Roeske J C, Bruland Ø S and Larsen R H 2003 Targeting of osseous sites with alpha-emitting 223Ra: comparison witn the Beta-Emitter 89Sr in Mice *J. Nucl. Med.* **44** 252–9

[37] Carrasquillo J A *et al* 2013 Phase I pharmacokinetic and biodistribution study with escalating doses of 223Ra-dichloride in men with castration-resistant metastatic prostate cancer *Eur. J. Nucl. Med. Mol. Imaging* **40** 1384–93

[38] Howell R W, Goddu S M, Narra V R, Fisher D R, Schenter R E and Rao D V 1997 Radiotoxicity of Gadolinium-148 and Radium-223 in Mouse testes: relative biological effectiveness of alpha-particle emitters *in vivo Radiat. Res.* **147** 342–8

[39] Unak P 2002 Targeted tumor radiotherapy *Brazilian Arch Biol Technol.* **45** 97–110

[40] Neves M, Kling A and Oliveira A 2005 Radionuclides used for therapy and suggestion for new candidates *J. Radioanal. Nucl. Chem.* **266** 377–84